



OPEN ACCESS

EDITED BY Jing Gao,

National Engineering Research Center for Oil Tea, China

REVIEWED BY Wenhui Yu,

Northeast Agricultural University, China

Jian Li,

Fujian Agriculture and Forestry University, China

Shaoiuan Liu.

South China Agricultural University, China

*CORRESPONDENCE

Peng Bin

☑ binpeng23@scau.edu.cn

RECEIVED 20 June 2025 ACCEPTED 28 August 2025 PUBLISHED 01 October 2025

CITATION

Wang K, Yang A, Li Y, Han Q, Yin Z, Xia S, Chen J, Mo J and Bin P (2025) *Artemisia argyi* essential oil modulates lipid metabolism via linoleic acid and glycerophospholipid pathways in high-fat diet-induced obese mice. *Front. Nutr.* 12:1650976. doi: 10.3389/fnut.2025.1650976

COPYRIGHT

© 2025 Wang, Yang, Li, Han, Yin, Xia, Chen, Mo and Bin. This is an open-access article distributed under the terms of the Creative Commons Attribution License (CC BY). The use, distribution or reproduction in other forums is permitted, provided the original author(s) and the copyright owner(s) are credited and that the original publication in this journal is cited, in accordance with accepted academic practice. No use, distribution or reproduction is permitted which does not comply with these terms.

Artemisia argyi essential oil modulates lipid metabolism via linoleic acid and glycerophospholipid pathways in high-fat diet-induced obese mice

Kaijun Wang^{1,2}, Anqi Yang², Yunxia Li³, Qi Han³, Zhangzheng Yin³, Siting Xia³, Jiayi Chen¹, Jiahao Mo² and Peng Bin^{1,4}*

¹Hunan Provincial Key Laboratory of the Traditional Chinese Medicine Agricultural Biogenomics, Changsha Medical University, Changsha, China, ²College of Animal Science and Technology, State Key Laboratory for Conservation and Utilization of Subtropical Agro-Bioresources, Guangxi University, Nanning, China, ³Animal Nutritional Genome and Germplasm Innovation Research Center, College of Animal Science and Technology, Hunan Agricultural University, Changsha, China, ⁴State Key Laboratory of Swine and Poultry Breeding Industry, Guangdong Laboratory of Lingnan Modern Agriculture, College of Animal Science, South China Agricultural University, Guangzhou, China

Obesity is a nutritional disorder caused by an imbalance between energy intake and expenditure. The natural products will provide hypolipidemic active factors that will intervene in obesity and its complications, as well as direct drug treatment. Artemisia argyi leaf is a well-known species in traditional Chinese medicine, and its essential oil (AAEO) has been identified to exert various physiological activities. This study investigates the chemical composition of essential oil extracted from Artemisia argyi (AAEO) and its potential effects on intestinal microbial function and lipid metabolism in mice subjected to a high-fat diet (HFD). The essential oil was extracted and analyzed for its bioactive compounds, revealing a rich presence of terpenes and oxygenated derivatives. Utilizing LC-MS/MS technology combined with multivariate statistical methods, significant alterations in serum metabolites were observed in AAEOtreated mice compared to those on HFD alone. Key metabolic pathways impacted by AAEO included linoleic acid metabolism and glycerophospholipid metabolism. These findings suggest that while AAEO did not significantly alter gut microbiota composition, it substantially modulated lipid metabolism via linoleic acid and glycerophospholipid pathways, suggesting a potential natural strategy for obesity-related metabolic disorders. This study provides new insights into the application of Artemisia argyi essential oil in dietary interventions and obesity management.

KEYWORDS

Artemisia argyi, high fat, essential oil, lipid, metabolomics

1 Introduction

The prevalence of obesity and the burden of obesity-related diseases are increasing worldwide. According to the World Health Organization (2023), over 1.9 billion adults worldwide are overweight or obese, with the prevalence continuing to rise (1). Obesity has also become a major public health problem in China. Obesity is characterized by excess

adipose tissue, an imbalance between energy intake and expenditure, and is associated with low-grade inflammation and insulin resistance, high fat induced obesity is also associated with atherosclerosis and nonalcoholic fatty liver disease (2-6). Dietary patterns in China have changed significantly compared to the last few decades, and there has been a gradual shift from a traditional plant-based fruit and vegetable diet to a Westernstyle diet, with an increasing intake of foods of animal origin, refined and processed grains, and foods high in sugar and fat (7). Consumption of ultra-processed foods was found to be associated with the risk of weight gain, overweight and obesity in a prospective study (8). There is also strong evidence that being overweight or obese is associated with an increased risk of major noncommunicable diseases (cardiovascular disease, type 2 diabetes and cancer) and premature death in the Chinese population (9-11). Therefore, improving obesity symptoms is imperative and important for intervening in the development of other diseases. Obesity is a complex multifactorial disease. The main causes of its pathogenesis include: environmental factors (mainly physical activity and diet), genetic factors, and gut microbes (12). Some anti-obesity medications, such as orlistat and lorcaserin, as well as phentermine/topiramate and naltrexone/bupropion extended-release tablets have been shown to be effective in reducing weight (13, 14). However, anti-obesity drugs may also lead to gastrointestinal problems, weakness, psychiatric disorders and cardiovascular diseases (15). Therefore, many experts predict that natural products will provide lipid-lowering active factors to intervene in obesity and its complications, as well as direct drug therapy.

Essential oil represents a large family, in which members are almost characterized by volatile and semi-volatile compounds, usually with a low molecular weight. It is generally formed as the secondary metabolite by aromatic plants (16). The chemical composition of essential oil can be categorized by their biosynthetic pathways as terpenes and their oxygenated derivatives (such as alcohols, ethers, aldehydes, ketones, and esters), and some aromatic and aliphatic compounds (16). Essential oil is traditionally obtained by steam or hydro-distillation (17–19). Recently, relatively new techniques, including solid-phase microextraction (SPME) (20), supercritical fluid extraction (SFE) (21), and microwave-assisted extraction (MAE) (22), have been developed and applied to collect these volatile constituents. Essential oil is reported to perform well in alleviating oxidative damage (23, 24), inflammation (25), infection (26, 27).

Artemisia argyi is an herbaceous plant distributed in most regions of East Asia. It has been widely used in traditional Chinese medicine for treating eczema, hemorrhage, and dysmenorrhea (28). Dried leaves of this herb are also used in acupuncture clinics in China to treat various diseases, especially chronic conditions such as osteoarthritis, asthma, gastrointestinal disorders, and insomnia (18). Artemisia argyi is reported to possess multiple pharmacological activities including anti-inflammatory, antimicrobial, antiasthma, analgesic, antivirus, antioxidant, antitumor and immunomodulatory effects (18, 29–31), most of which are contributed by the essential oil existing in Artemisia argyi leaves. Artemisia argyi is a rich source of essential oil (AAEO), ~1.13% (w/w) (18). Indeed, the strong and aromatic odors of

Artemisia argyi are mostly attributed to a high concentration of essential oil. With the help of gas chromatography-mass spectrometry (GC–MS), a total of 33 compounds were initially identified in AAEO, and eucalyptol, also known as 1,8-cineole, was most plentiful, accounting for 23.66% (29). However, the amount of 1,8-cineole was quantified to 33.4% in another study (17). By comparing the phytochemicals of AAEO from eight different areas, locality was considered as a factor affecting the quality of AAEO (32). AAEO has been relatively little studied, although it is a terrestrial herb. The objective of this study was to investigate the chemical composition of AAEO and the effects on gut microbial function and serum metabolic profiles in a mouse model of diet-induced obesity. A systematic study was conducted using ICR mice to determine the alterations in microbial function and serum differential metabolites of AAEO with obesity.

2 Materials and methods

2.1 Volatile oil obtaining

The volatile oil was isolated by hydrodistillation at the Jiangxi Hairui Natural Plant Co., Ltd. (Jian, China). The leaves of *Artemisiae Argyi* were air-dried before steam distillation. The AAEO after extraction was stored in sealed amber ampules at 4 °C until being tested or analyzed.

2.2 GC-MS analysis

The volatile oil was analyzed on a GCMS-QP2010 Plus Mass Spectrometer (Shimadzu) equipped with a DB-5 ms capillary column (30.0 m \times 0.25 mm; film thickness, 0.25 μm) and mass spectrometry MS detector (MS). GC conditions were the same as described above), and data were recorded in the full-scan acquisition mode with the range of m/z 45–500. The compounds were identified by comparing retention indices (RI) and mass spectra with data from the NIST 11.0 MS library and the literature.

2.3 Experimental animals

Animal experiments were conducted in accordance with the Hunan Agricultural University Institutional Animal Care and Use Committee (202105). Six-week-old male ICR mice were purchased from SLAC Laboratory Animal Central (Changsha, China). A total of 50 male mice (29.40 \pm 1.23 g) were divided into 5 groups at random and housed in polypropylene cages and maintained in standard laboratory conditions of temperature (25 \pm 2 $^{\circ}$ C) and light-dark cycle (12 h/12 h). The diets of mice were fed the control diet (Con), the high-fat diet (HFD), and the HFD-fed mice with the low (LEO, 0.20 ml/kg), medium (MEO, 0.40 ml/kg), and high (HEO, 0.80 ml/kg) doses of AAEO as previous study (33). AAEO dissolved in 4% Tween 80 and administered by gastric administration. Before any treatment, mice were housed for 7 days to allow adaptation. The experiment lasted for 8 weeks. At the end of the experiment the animals were sacrificed under anesthesia.

2.4 Fecal collection and sequencing

Prepare 1.5 ml sterile centrifuge tubes (marked animal number in advance), sterile forceps, and transfer the mice to a clean, sterile individual feeding cage after 8 hours on an empty stomach. Pick up fresh stool directly with sterile forceps, avoiding hand contact with the sample. Dispense into marked sterile centrifuge tubes immediately after collection and place kept at $-80~^{\circ}\text{C}$ for examination. The fecal DNA extraction and 16S ribosomal RNA amplification were conducted as previously reported (34, 35). The microbial function prediction analysis process refers to previous studies (36, 37).

2.5 Serum metabolite extraction and quality control sample

100 µl serum sample was added to a 1.5 ml centrifuge tube with 400 μ l solution [acetonitrile: methanol = 1:1(v:v)] containing 0.02 mg/ml internal standard (L-2-chlorophenylalanine) to extract metabolites. The samples were mixed by vortex for 30 s and lowtemperature sonicated for 30 min (5 °C, 40 KHz). The samples were placed at -20 °C for 30 min to precipitate the proteins. Then the samples were centrifuged for 15 min (4 °C, 13,000 g). The supernatant was removed and blown dry under nitrogen. The sample was then re-solubilized with 100 µl solution (acetonitrile: water = 1:1) and extracted by low-temperature ultrasonication for 5 min (5 °C, 40 KHz), followed by centrifugation at 13,000 g and 4 °C for 10 min. The supernatant was transferred to sample vials for LC-MS/MS analysis. As a part of the system conditioning and quality control process, a pooled quality control sample (QC) was prepared by mixing equal volumes of all samples. The QC samples were disposed and tested in the same manner as the analytic samples. It helped to represent the whole sample set, which would be injected at regular intervals (every 5 samples) in order to monitor the stability of the analysis.

2.6 Serum metabolomics analysis

The LC-MS/MS analysis of sample was conducted on a Thermo UHPLC-Q Exactive HF-X system equipped with an ACQUITY HSS T3 column (100 mm \times 2.1 mm i.d., 1.8 μ m; Waters, USA) at Majorbio Bio-Pharm Technology Co. Ltd. (Shanghai, China). The mobile phases consisted of 0.1% formic acid in water: acetonitrile (95:5, v/v) (solvent A) and 0.1% formic acid in acetonitrile: isopropanol:water (47.5:47.5, v/v) (solvent B). The flow rate was 0.40 ml/min and the column temperature were 40 °C. The injection volume was 3 µl. The mass spectrometric data were collected using a Thermo UHPLC-Q Exactive HF-X Mass Spectrometer equipped with an electrospray ionization (ESI) source operating in positive mode and negative mode. The optimal conditions were set as followed: Aux gas heating temperature at 425 °C; Capillary temp at 325 °C; sheath gas flow rate at 50 psi; Aux gas flow rate at 13 psi; ion-spray voltage floating (ISVF) at -3,500 V in negative mode and 3,500 V in positive mode, respectively; Normalized collision energy, 20-40-60 eV rolling for MS/MS. Full MS resolution was 60,000, and MS/MS resolution was 7,500. Data acquisition was performed with the Data Dependent Acquisition (DDA) mode. The detection was carried out over a mass range of 70–1,050 m/z.

2.7 Statistical analysis

Statistical analyses between the means of each group were analyzed using one-way ANOVA (one-way analysis of variance) followed by Duncan comparison range tests through SPSS 22.0. The statistical significance level was set at p < 0.05. The significance between groups represented by * was p < 0.05, ** represented p < 0.01, *** represented p < 0.001. For the metabolomics data, the raw data were imported into the Progenesis QI software (Waters Corporation, Milford, USA) for data preprocessing after UHPLC-QE-HFX/MS analyses. Through baseline filtering, peak identification, peak integral, retention time correction, and peak alignment. Then, the data matrix containing sample names, m/z, retention time and peak intensities was exported for further analyses. At the same time, the metabolites were identified by searching database, and the main databases were the HMDB (https://www.hmdb.ca), Metlin (https:// metlin.scripps.edu/) and the self-compiled Majorbio Database (MJDB) of Majorbio Biotechnology Co., Ltd. (Shanghai, China). The R package "ropls" (Version 1.6.2) was used to perform principal component analysis (PCA) and orthogonal least partial squares discriminant analysis (OPLS-DA), and 7-cycle interactive validation evaluating the stability of the model. The metabolites with VIP > 1, p < 0.05 were determined as significantly different metabolites based on the Variable importance in the projection (VIP) obtained by the OPLS-DA model and the p-value generated by student's t test.

3 Results

3.1 Essential oil composition

The chemical composition of AAEO was analyzed by GC/MS as shown in Table 1. Only components with concentrations >0.3% are reported. The obtained results indicated the presence of 25 chemical compounds in the chromatogram, constituting 90.79% of the total components detected. The highest compositions of the compounds were 18.43% of Linalool, followed by Bicyclo[2.2.1] heptan-2-one, 1,7,7-trimethyl-, (1S)- (13.28%), Safroleb (11.96%), D-Limonene (10.86%), Tricyclo[2.2.1.0(2, 6)]heptane, 1,7-dimethyl-7-(4-methyl-3-pentenyl)-, (-)- (6.78%), 3-Cyclohexene-1-methanol, alpha.,4-trimethyl-, (R)- (5.53%), and alpha-Terpineol (5.38%).

3.2 Fecal microbial function prediction

As demonstrated in Figure 1, based on PICRUSt prediction, the microbiota function was predicted; the KEGG pathway in top 10 at level 2 about metabolism included global and overview maps, carbohydrate metabolism, amino acid metabolism, energy metabolism, metabolism of cofactors and vitamins, and nucleotide

TABLE 1 Chemical constituents of AAEO identified by GC-MS.

Peak no	R_t^{1}	Compound	Area%
1	14.165	alpha-Pinene	1.07
2	15.023	Bicyclo[3.1.0]hexane, 4-methylene-1-(1-methylethyl)-	1.45
3	15.161	beta-Pinene	0.77
4	15.276	beta-Myrcene	1.06
5	16.421	D-Limonene	10.86
6	16.488	Eucalyptol	2.25
7	16.79	gamma-Terpinene	0.46
8	17.05	trans-Linalool oxide (furanoid)-	0.3
9	17.394	Cyclohexene, 3-methyl-6-(1-methylethylidene)-	0.41
10	18.154	Linalool	18.43
11	19.284	Bicyclo[2.2.1]heptan-2-one, 1,7,7-trimethyl-, (1S)-	13.28
12	19.739	endo-Borneol	0.48
13	19.905	3-Cyclohexen-1-ol, 4-methyl-1-(1-methylethyl ethyl)-, (R)-	2.66
14	20.273	3-Cyclohexene-1-methanol, alpha, 4-trimethyl-, (R)-	5.53
15	20.288	alpha-Terpineol	5.38
16	22.86	Safrole	11.96
17	24.422	Phenol, 2-methoxy-3-(2-propenyl)-	1.83
18	24.969	2,6-Octadien-1-ol, 3,7-dimethyl-, acetate, (Z)-	0.33
19	25.408	Copaene	0.88
20	25.949	Methyleugenol	0.78
21	27.231	Tricyclo[2.2.1.0(2,6)]heptane, 1,7-dimethyl-7-(4-methyl-3-pentenyl)-, (-)-	6.78
22	27.586	transalphaBergamotene	1.22
23	28.732	Humulene	0.51
24	29.638	Germacrene D	0.47
25	32.404	1,6,10-Dodecatrien-3-ol, 3,7,11-trimethyl-, (E)-	1.64

 $^{{}^{1}}R_{t}$, retention time (min).

metabolism et al. in three dietary treatments (Figure 1A). Totally, the PICRUSt predicted 295 pathways in level 3 of fecal samples, among them, only 80 pathways were related to metabolism (level 2). The central pathway in top 10 of level 3 contained five pathways about global and overview maps (as shown in Figure 1B), which were metabolic pathways, biosynthesis of secondary metabolites, microbial metabolism in diverse environments, biosynthesis of amino acids, and carbon metabolism respectively. In addition, the pathways of amino sugar and nucleotide sugar metabolism, glycolysis/gluconeogenesis, starch and sucrose metabolism were associated with carbohydrate metabolism. The purine metabolism and pyrimidine metabolism were associated with nucleotide metabolism at level 3. Finally, the top 10 pathways in KEGG

levels 2 and 3 were not notably different (p > 0.05). Analysis of the AAEO's effects on the mouse fecal microbiota demonstrated that it influenced the functional potentials of these microbes (Table 2). Compared to the Con group, the HFD group with AAEO significantly raised (p < 0.05) abundance of lysine biosynthesis, tyrosine metabolism, pyruvate metabolism, and glycerolipid metabolism related with amino acid, carbohydrate, and lipid metabolism. On the contrary, the HFD group with AAEO significantly decreased (p < 0.05) abundance of phenylpropanoid biosynthesis, pentose and glucuronate interconversions, oxidative phosphorylation, carbon fixation pathways in prokaryotes, and cyanoamino acid metabolism than Con group. Although HFD significantly increased the abundance of the other glycan degradation pathway associated with glycan biosynthesis and metabolism (p < 0.05), the addition of AAEO to HFD had no effect on it (p > 0.05).

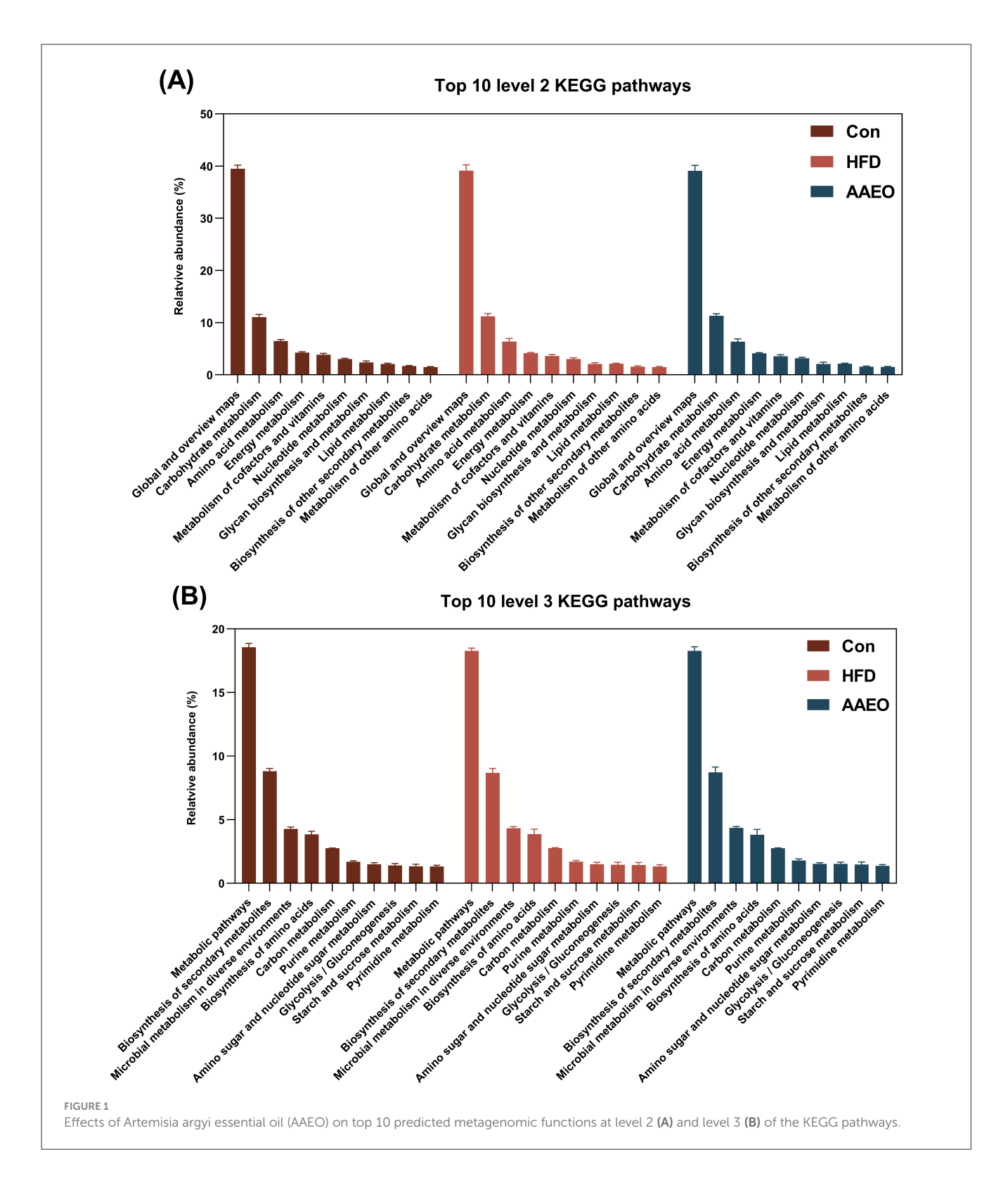
3.3 Data quality control and identified metabolites

The QC sample positive (Figure 2A) and negative (Figure 2B) ion assessment plots were shown in Figure 2. A QC sample was injected every eight samples to verify the system stability during the whole sample batch. For the overall data, the RSD $\,<\,0.3$ and the percentage of peak accumulation >70% indicated that the proposed method was stable, and the overall data measured were qualified (dashed line indicates before pretreatment, solid line indicates after pretreatment). It can be seen that when the RSD was 30%, the peak accumulation percentages of positive ions and negative ions of QC samples are 95.8% and 95.2% respectively. It indicated that the data is stable and reliable and can be used for subsequent analysis. The metabolite classification information obtained based on the identification of HMDB database is shown in Figure 2C. It can be proved that the metabolite species of mice blood were mainly concentrated in lipids and lipidlike molecules, organic acids and derivatives, organoheterocyclic compounds, benzenoids, and phenylpropanoids and polyketides. Lipids and lipid-like molecules were the most abundant metabolites with 239, followed by organic acids and their derivatives with 124.

As shown in Table 3, a total of 7,107 positive ion mass spectrometry peaks and 5,106 negative ion mass spectrometry peaks were identified by LC-MS/MS non-targeted metabolomics; 357 positive ion metabolites and 243 negative ion metabolites compared to public databases; and 173 positive ion metabolites and 102 negative ion metabolites compared to KEGG database.

3.4 PCA and PLS-DA analysis

In order to better understand and analyze the intervention effect of AAEO on blood metabolites in mice on HFD, the blood metabolite data from each group of mice were analyzed by PCA in this study. From Figure 3, it can be seen that there was a trend of separation between the samples of mice in the HFD group and those of mice in the AAEO group regardless of the



positive (Figure 3A) or negative (Figure 3B) ion mode, indicating that AAEO affected the changes of metabolites in the blood of mice. Between the mice in the Con group and the samples from the HFD group, there was a greater degree of separation within the groups, and there was a crossover between the groups, and the differences were not significant. This may be due to the fact that

there were more factors that have an impact on the data, i.e., not only the dietary factors set up in this experiment, but also individual differences in mice, the stability of the instrumentation, and other external factors, resulting in the phenomenon of underfitting the data, and therefore the PLS-DA statistical method is needed to continue the analysis, and thus to ignore the random differences

TABLE 2 KEGG pathways that showed different abundances between fecal microbiota by fed AAEO.

Level 2	Level 3	Pathway ID	Con ¹	HFD ²	AAEO ³
Amino Acid Metabolism	Lysine biosynthesis	ko00300	$0.56\pm0.04^{\text{b}}$	0.58 ± 0.05^{ab}	0.63 ± 0.06^{a}
	Tyrosine metabolism	ko00350	0.17 ± 0.02^{b}	0.18 ± 0.02^{ab}	0.19 ± 0.01^{a}
Biosynthesis of other secondary metabolites	Phenylpropanoid biosynthesis	ko00940	0.17 ± 0.03^{a}	0.14 ± 0.03^{ab}	0.12 ± 0.05^{b}
Carbohydrate metabolism	Pyruvate metabolism	ko00620	1.01 ± 0.04^{b}	1.04 ± 0.06^{ab}	1.08 ± 0.05^{a}
	Pentose and glucuronate interconversions	ko00040	0.38 ± 0.06^{a}	0.34 ± 0.09^{ab}	0.30 ± 0.06^{b}
Energy metabolism	Oxidative phosphorylation	ko00190	1.00 ± 0.09^{a}	0.93 ± 0.05^{ab}	0.91 ± 0.09^{b}
	Carbon fixation pathways in prokaryotes	ko00720	0.93 ± 0.05^a	0.88 ± 0.05^{ab}	$0.84\pm0.08^{\text{b}}$
Glycan Biosynthesis and Metabolism	Other glycan degradation	ko00511	0.49 ± 0.10^{a}	0.37 ± 0.07^{b}	$0.37 \pm 0.12^{\text{b}}$
Lipid Metabolism	Glycerolipid metabolism	ko00561	0.36 ± 0.07^{b}	0.42 ± 0.05^{ab}	0.44 ± 0.06^{a}
Metabolism of other amino acids	Cyanoamino acid metabolism	ko00460	0.33 ± 0.03^{a}	0.29 ± 0.03^{ab}	$0.28\pm0.04^{\text{b}}$

 $^{^{1}}$ Con, control diet; 2 HFD, high fat diet; 3 AAEO, high fat diet with HEO. In the same row, values with no letter or the same letter superscripts mean no significant difference (p > 0.05), while with different small letter superscripts mean significant difference (p < 0.05).

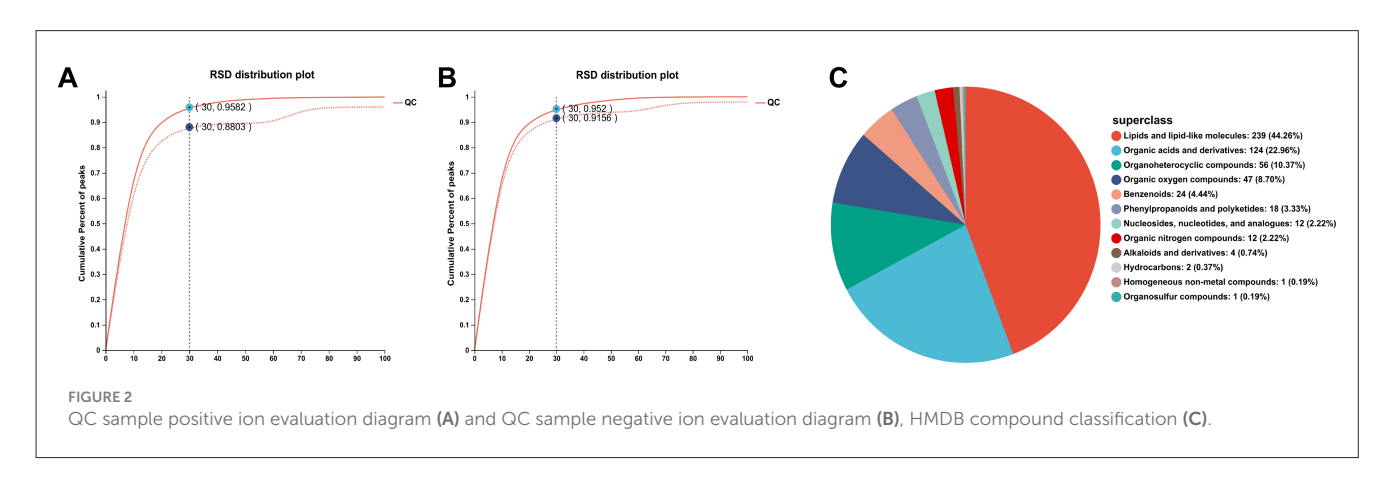


TABLE 3 Total ions and identification statistics chart.

lon mode	All peaks ³	Identified metabolites	Metabolites in library	Metabolites in KEGG
Pos ¹	7107	471	357	173
Neg ²	5106	314	243	102

 $^{^1}$ Pos, positive ionization mode, 2 Neg, negative ion mode; 3 All peaks, number of mass spectral peaks extracted by the software.

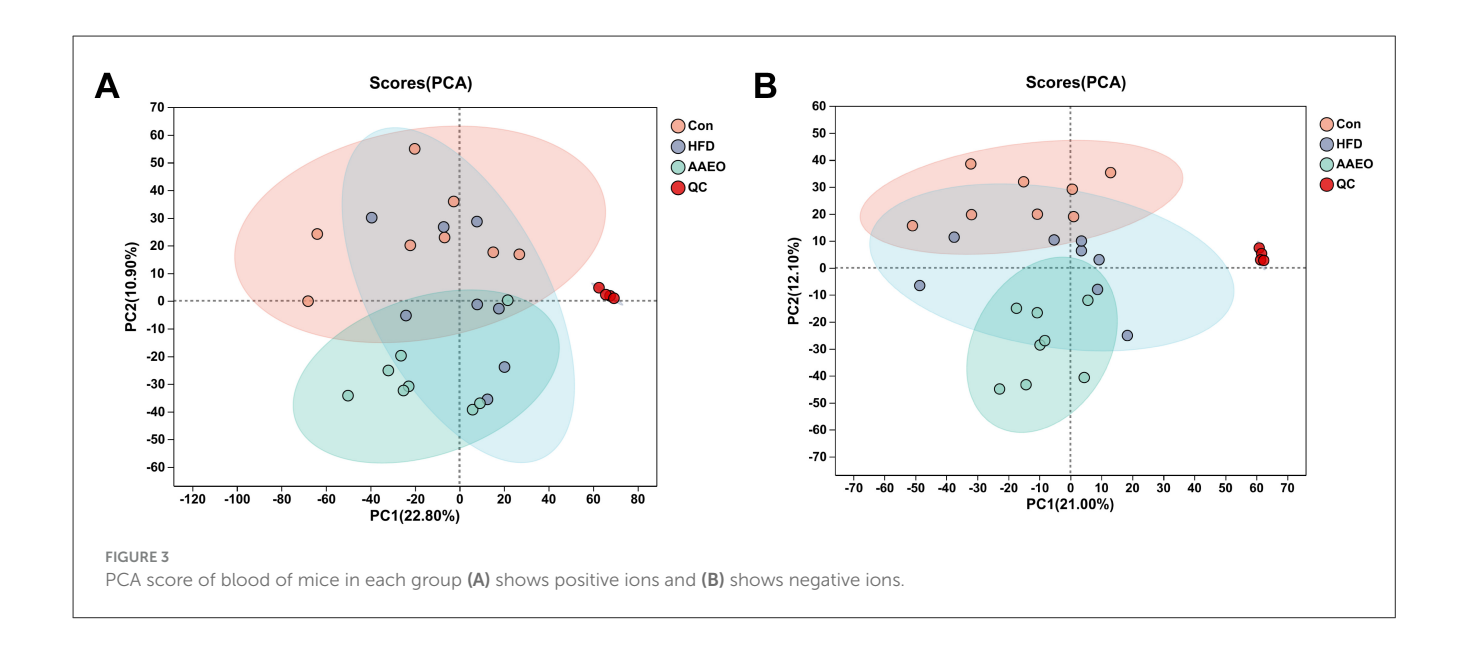
within the groups and to highlight the systematic differences between the groups.

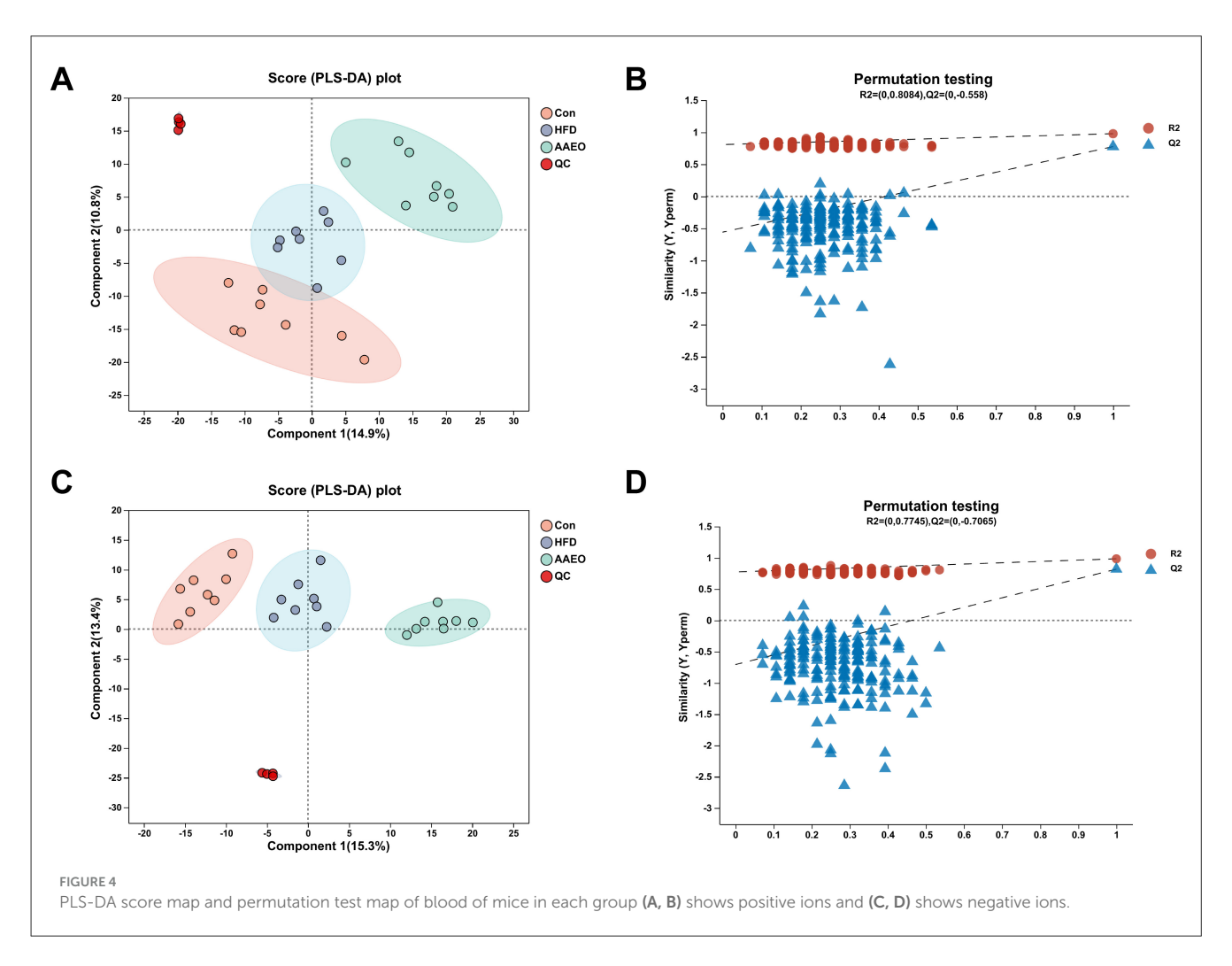
As can be shown from Figures 4A, C, there was no crossover between the samples of the Con group and HFD in either the positive or negative ion mode, and the degree of separation was good. There was no crossover or overlap between the samples of the HFD group and AAEO group. It indicated that the AAEO has a significant effect on the metabolites in the blood of mice on HFD. The replacement test graph was used to speculate whether the model was reliable or not, and the criterion for the evaluation of the replacement test was mainly the intercept of the Q^2 regression line with the Y-axis, when the intercept was <0.05, it indicated that the model was robust and reliable. As shown in Figures 4B, D, $Q^2 = -0.558 < 0.05$ in the positive ion model and $Q^2 = -0.7065 < 0.05$

in the negative ion model, indicating that the model was robust and reliable without overfitting in either ion model.

3.5 OPLS-DA analysis

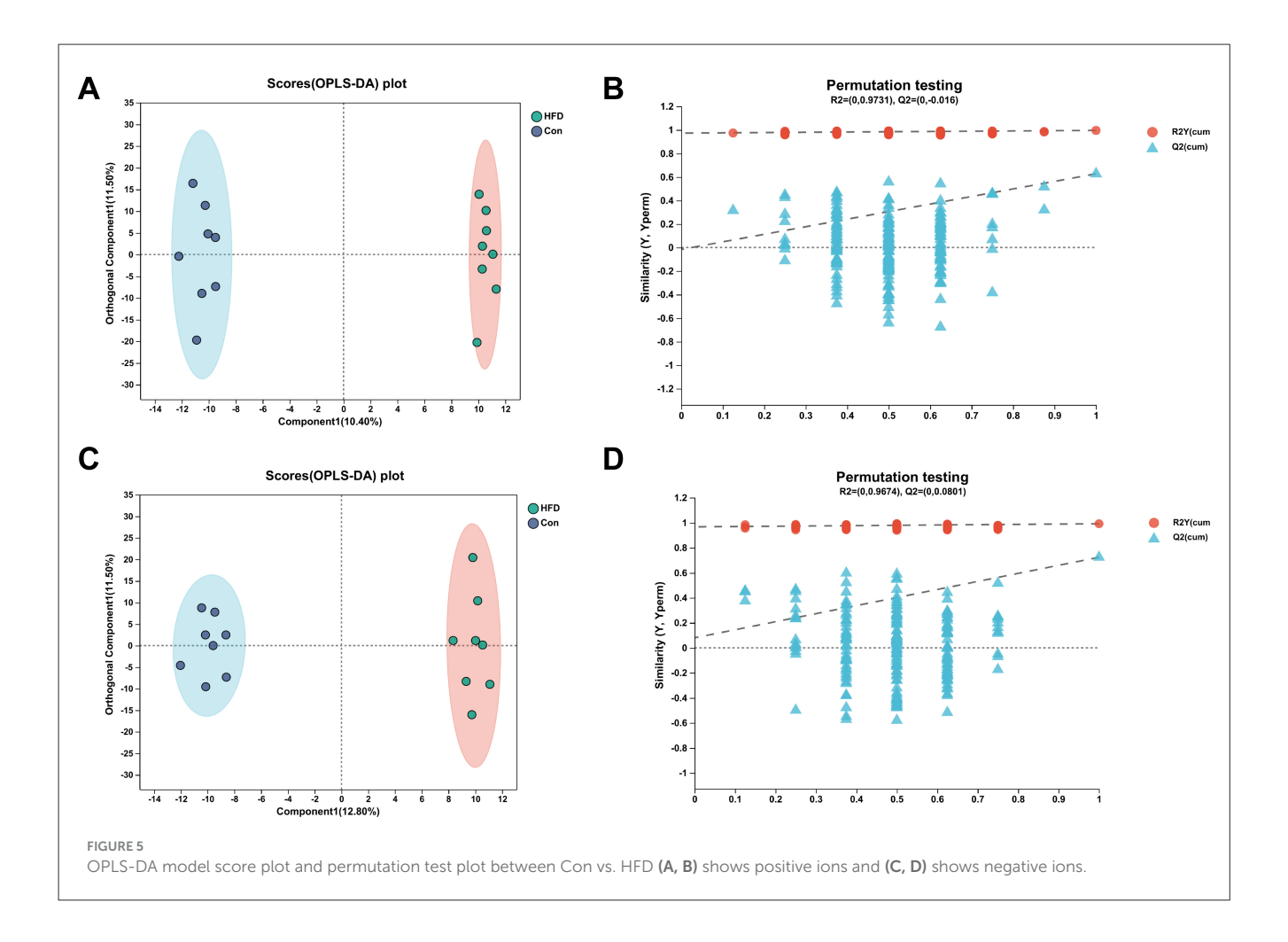
Orthogonal Partial Least Squares Discriminant Analysis, OPLS-DA was a derivative of PLS-DA. OPLS-DA can better distinguish between subgroups and improve the validity and parsing ability of the model. The OPLS-DA model score plot and permutation test plot between Con vs. HFD and HFD vs. AAEO were shown in Figures 5, 6A, C, respectively, and there was a clear trend of separation between Con vs. HFD and between HFD vs. AAEO in both positive and negative ion modes. And from Figures 5B, D, Q^2 was <0.05 in the positive ion mode, and Q^2 was >0.05 in the negative ion mode, and with the decrease of replacement retention in the negative ion mode, R2 and Q2 decreased, and the regression line showed an upward trend, which could indicate that the replacement test was passed, and the model did not have the overfitting phenomenon. From Figures 6B, D, it could be proved that Q^2 is <0.05 in both the positive ion mode and the negative ion mode, indicating that the model was robust and reliable without overfitting in either ion mode.





The parameters of the OPLS-DA models for positive and negative ionization were listed in Table 4. The closer the R^2Y and Q^2 were to 1, the more stable and reliable the model was, $Q^2 > 1$

0.5 indicated a better predictive ability of the model, and $Q^2 <$ 0.5 indicated a poorer predictive ability of the model. As can be seen from the table, the cumulative explanatory rate of $R^2 Y$ for



the comparison between the two groups in both the positive and negative ion modes exceed 0.9, indicating that at least 90% of the variance in the Y-measure can be explained by these OPLS-DA models. The Q^2 calculated by cross-validation showed that the predictions of the OPLS-DA models were good for all groups. In particular, the R^2Y and Q^2 between the Con vs. HFD groups were close to 1, indicating that the HFD-induced obesity model in this study, modeling was successful. In addition, $Q^2 > 0.5$ between the HFD vs. AAEO groups indicated that ingestion of AAEO could successfully modulate the metabolite composition caused by HFD.

3.6 Screening and identification of differential metabolites between different groups

Screening was performed based on the variable importance of projection (VIP) analysis obtained from the OPLS-DA model. Metabolites with VIP value >1 and p-value <0.05 were considered as significantly different metabolites between the two groups. Table 5 showed the number of significantly different metabolites from the comparative analysis between the two groups. A total of

170 significantly different metabolites were identified in the positive ion mode and 156 significantly different metabolites were identified in the negative ion mode. Compared with the Con group, there were 79 significantly different metabolites in the positive ion mode and 68 in the negative ion mode in the HFD group, and 123 significantly different metabolites in the positive ion mode and 127 in the negative ion mode in the AAEO group. Compared with HFD, there were 91 significantly different metabolites in positive ion mode and 78 significantly different metabolites in negative ion mode in the AAEO group.

Supplementary Table S1 showed the significantly different metabolites in the Con group compared with the HFD group screened according to VIP > 2 and p-value < 0.05. A total of 60 significantly different metabolites were identified, including six amino acids, peptides, and analogs, four fatty acids and conjugates, two glycerophosphocholines, two bile acids, alcohols and derivatives, one glycerophosphocholines, five carbohydrates and carbohydrate conjugates, and so on. Based on the abundance of metabolites after normalized treatment, 10 metabolites were found to be significantly up-regulated (P < 0.05) and 50 metabolites were found to be significantly down-regulated (P < 0.05) in the HFD group compared with Con group.

Supplementary Table S2 showed the significantly different metabolites in the AAEO group compared with the HFD group

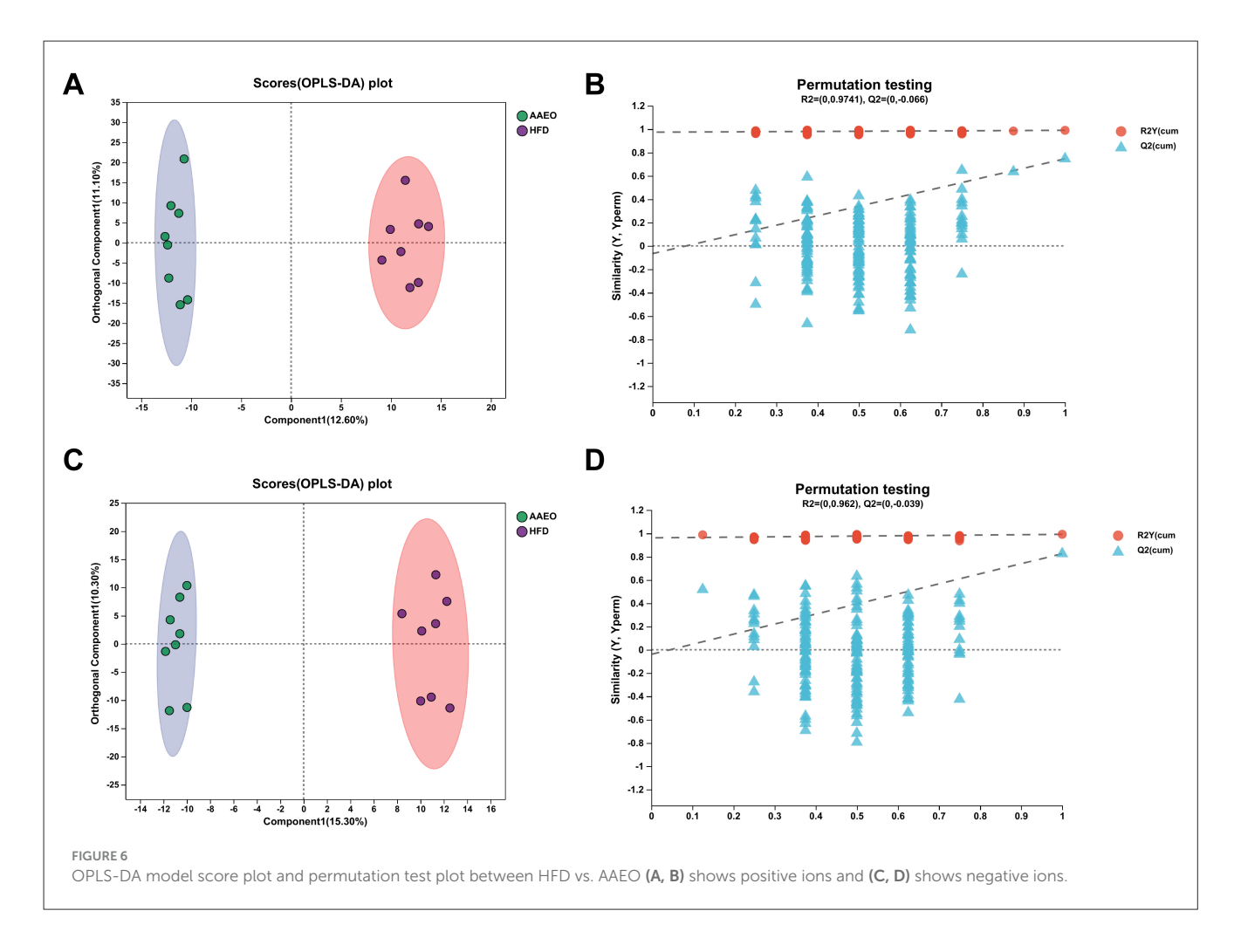


TABLE 4 OPLS-DA model parameters.

Group	lon mode	R ² X (cum)	R ² Y (cum)	Q ² (cum)
Con vs. HFD	vs. HFD Positive ion		0.996	0.627
	Negative ion	0.243	0.992	0.724
HFD vs. AAEO	Positive ion	0.237	0.990	0.746
	Negative ion	0.256	0.992	0.826

 R^2X and R^2Y denote the explanatory rates of the constructed model for the X and Y matrices, respectively, and R^2X (cum) and R^2Y (cum) denote the cumulative explanatory rates; Q^2 denotes the predictive power of the model.

according to the VIP > 2 and p-value < 0.05 screening. A total of 79 significantly different metabolites were identified, including six Amino acids, peptides, and analogs, four fatty acids and conjugates, three fatty acyl glycosides, three carbohydrates and carbohydrate conjugates, two triterpenoids, and three terpene glycosides, and others. Based on the abundance of metabolites after normalized treatments, 22 metabolites were found to be significantly upregulated (P < 0.05) and 57 metabolites were found to be significantly down-regulated (P < 0.05) in the AAEO group as compared to HFD group.

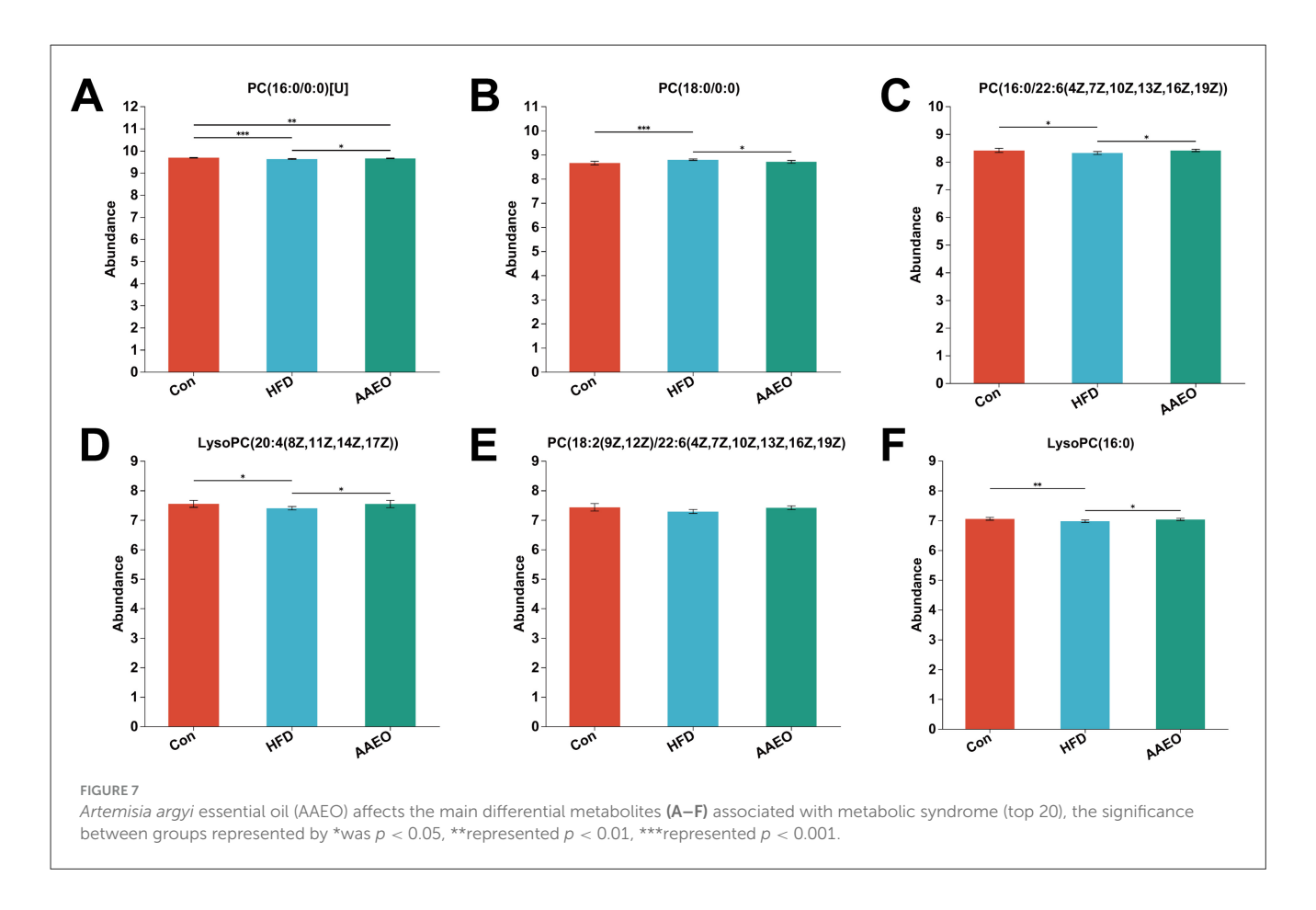
TABLE 5 The number of metabolites with significant difference.

Mode	Total number	Con ¹ _vs_ HFD ²	HFD_vs_ AAEO ³	Con_vs_ AAEO
Pos	1,534 (170)	611 (79)	693 (91)	958 (123)
Neg	1,233 (156)	554 (68)	557 (78)	878 (127)

Numbers in parentheses represent the number of named differential metabolites identified. 1 Con, control diet; 2 HFD, high fat diet; 3 AAEO, high fat diet with HEO.

3.7 Differential metabolite analysis for multiple comparisons

The major differential metabolites of AAEO associated with obesity screened according to the Kruskal–Wallis rank sum test are shown in Figure 7. The most abundant differential metabolite was PC (16:0/0:0) [U] (Figure 7A), which was significantly lower in the HFD group than in the Con group (P < 0.05), and it was significantly elevated by AAEO intake (P < 0.05). However, the content of PC (18:0/0:0) in the HFD group was significantly higher than that in the Con group (P < 0.05), and the intake of AAEO significantly decreased its content (Figure 7B) (P < 0.05). In addition, PC [16:0/22:6(4Z,7Z,10Z,13Z, 16Z,19Z)], LysoPC [20:4(8Z,11Z,14Z,17Z)], PC [18:2(9Z,12Z)/22:6



(4Z,7Z,10Z,13Z,16Z,19Z)], and LysoPC (16:0) were significantly lower than those in the Con group and were restored after AAEO ingestion (P < 0.05) (Figures 7C–F).

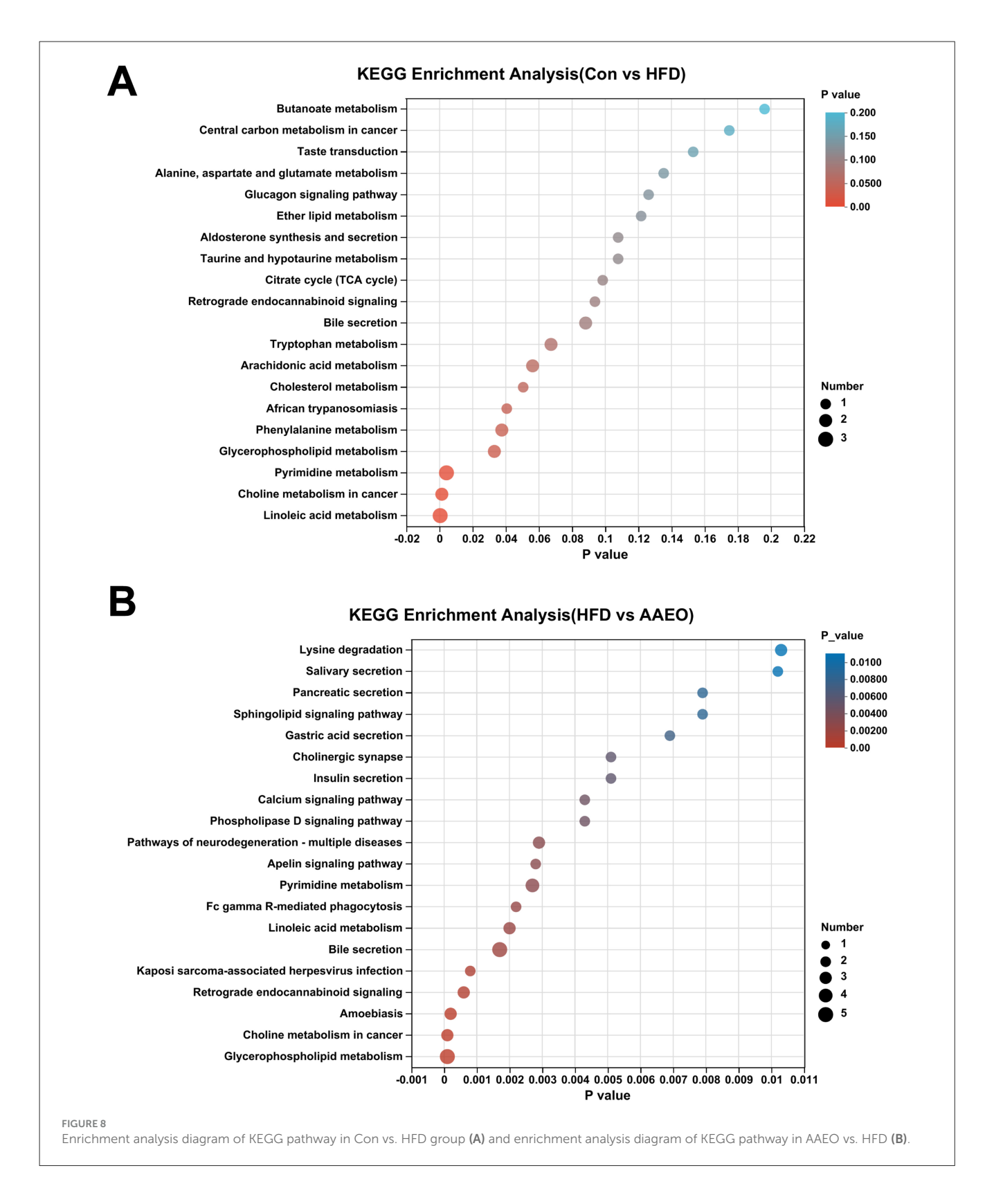
3.8 Enrichment analysis of KEGG functional pathways for differential metabolites

Based on the difference metabolites between the two groups screened earlier, the KEGG pathway enrichment in each group was further screened by using the calculation method of num in study/num in pop. The KEGG pathway enrichment in the Con vs. HFD group and the AAEO vs HFD group was shown in Figure 8. It was shown in Figure 8A by analyzing the KEGG pathways in the Con vs. HFD group, we can obtain that there were 20 major pathways enriched. There were 20 major enriched pathways. Among them, linoleic acid metabolism, pyrimidine metabolism, glycerophospholipid metabolism and phenylalanine metabolism were significantly higher than other metabolic pathways (P < 0.05). In addition, some of them focused on the metabolic pathways of fat metabolism regulation, such as cholesterol metabolism, and fatty acid metabolism pathways, such as arachidonic acid metabolism. As shown in Figure 8B, there were 20 major enriched pathways by analyzing the KEGG pathways in the AAEO vs. HFD group. Glycerophospholipid metabolism had the highest enrichment rate and was significantly higher than other pathways (P < 0.05). This was followed by retrograde endocannabinoid signaling, bile secretion, linoleic acid metabolism, Fc gamma *R*-mediated phagocytosis, pyrimidine metabolism and apelin signaling pathway. Two of them were the main pathways involved in lipid metabolism, including glycerophospholipid metabolism and linoleic acid metabolism.

4 Discussion

Medicinal plants are nature's gift to human beings to help them battle against various ailments since thousands of years ago. Now with the globalization of pursuing improved quality of life, there is actually a general rising tendency in demand for dietary function plants in the world (38). A report from the World Health Organization (WHO) disclosed that almost 80% of the world's population relies on nonconventional drug-treatment, particularly of medicinal herb, in their primary healthcare (39). However, although great progress is being made in uncovering the chemistry and bioactivities of functional food plants, their exact biological functions and regulation mechanisms largely remain to be elucidated.

Artemisia argyi was used as a traditional remedy for various diseases in Asia, modern studies have proved its modulatory effects on the inflammation process such as rhinitis, dermatitis and arthritis, furthermore, preparation of the essential oil has been clinically prescribed for chronic bronchitis in China for years (40, 41). GC-MS analysis in this study provided detailed chemical composition of AAEO, in which several predominant chemicals



including cineole, borneol, camphor, and thujone were found to possess anti-inflammatory activities according to previous reports (42, 43). These reports imply that AAEO may be associated with anti-inflammatory properties due to the presence of the above components. The key metabolic pathways identified—linoleic acid

metabolism and glycerophospholipid metabolism—are critical for lipid homeostasis. Linoleic acid, an essential fatty acid, undergoes desaturation and elongation to form bioactive lipid mediators (e.g., prostaglandins) that regulate inflammation and adipocyte function (43). Our data show that AAEO normalizes linoleic acid-derived

metabolites disrupted by HFD, suggesting AAEO may mitigate HFD-induced lipid dysregulation by restoring balanced production of these mediators. The chemical composition of the essential oil of *Artemisia argyi* aerial parts in the present study was not the same as that reported in previous studies. For example, eucalyptol, (-)-camphor and viridiflorol were the main volatile compo nents of *Artemisia argyi* from Zunyi City, Guizhou Province, China, moreover, the content and composition of the volatile oil of *Artemisia argyi* were various with different growing period (44). However, eucalyptol, camphor, and caryophyllene were common constituents in *Artemisia argyi* (45, 46). These differences of chemical content and composition of the essential oils might have been due to harvest time and local, climatic and seasonal factors as well as storage duration of medicinal herbs, and these differences may result in different biological activities.

High-throughput sequencing technology had many advantages. It can not only accurately analyze the structure and diversity of gut microbiota, but also further predict the gene functions and metabolic pathways of intestinal microorganisms (47, 48). The functional composition of the metagenome was predicted by PICRUSt using marker gene data and a reference genome database obtained from 16S rRNA sequencing. The results of gut microbiota showed that the microbes were mainly involved in global and overview maps, carbohydrate metabolism, amino acid metabolism and energy metabolism. According to the results of intestinal microbial function prediction, we anticipated that AAEO would not widely alter gut and fecal microbiota function.

The rapid development of metabolomics technology has become an important research tool in the fields of clinical medicine, life sciences, and food science (49, 50). Metabolomics techniques are used to study the changes in active food ingredients during food production, processing, and storage processes, and to investigate their precise mechanisms after ingestion. In addition, the application of metabolomics in analyzing interactions between different species not only provides a broad metabolic pathway, but also explains the mechanisms of microbial host interactions, playing a key role in systems biology (51). A series of open platforms currently used for metabolomics data analysis, including convenient and complete metabolomics databases such as Kyoto Encyclopedia of Genes and Genomes (KEGG), Max library database, Metabolites and Chemical Entities (METLIN) database, and Human Metabolomics Database (HMDB), provide a sustainable information sharing platform. In order to better understand and analyze the intervention effect of AAEO on serum metabolites in HFD mice. The dose-dependent efficacy of AAEO (HEO > MEO > LEO) in regulating lipid metabolism was supported by preliminary biochemical indicators data, reinforcing that the HEO group was the optimal dose for exploring the underlying mechanisms. This study conducted PCA analysis on the serum metabolite data of mice in each group. There was a clear separation trend between the control group mice and the HFD group mice samples, indicating that HFD can affect the changes in substances in mouse serum. Similarly, AAEO can also affect changes in metabolites in the serum of HFD mice. OPLS-DA can better distinguish differences between groups, improve the effectiveness and parsing ability of the model. According to PCA and PLS-DA analysis, regardless of the ion mode, it has been proven that the model is robust and reliable, and no overfitting has occurred.

This study used LC-MS/MS technology combined with multivariate statistical methods to analyze the effect of AAEO on the metabolomics of HFD induced obese mice and screened for multiple significantly different metabolites. The results indicated that AAEO can significantly regulate diet, especially metabolic abnormalities caused by HFD. 60 and 79 significantly different metabolites were screened from the HFD and AAEO groups based on VIP > 2 and p < 0.05, respectively. Six significantly different metabolites related to AAEO regulation of obesity were selected through multiple group comparisons, including PC (16:0/00:0), PC (18:0/0:0) PC [16:0/22:6(4Z,7Z,10Z,13Z,16Z,19Z)], LysoPC [20:4(8Z,11Z,14Z,17Z)], PC [18:2(9Z,12Z)/22:6(4Z,7Z, 10Z,13Z,16Z,19Z)], and LysoPC (16:0). In addition, the pathway regulating lipid metabolism by AAEO were mainly enriched in linoleic acid metabolism and glycerophospholipid metabolism. For glycerophospholipid metabolism, the observed changes phosphatidylcholines (PCs) and lysophosphatidylcholines (LysoPCs) are biologically meaningful: PCs are major components of cell membranes and serve as precursors for triglyceride transport, while LysoPCs are involved in lipid signaling and fatty acid uptake (52). AAEO's restoration of these metabolites [e.g., increased PC (16:0/0:0) and decreased PC (18:0/0:0) in treated mice] indicates potential modulation of membrane integrity and triglyceride trafficking, processes central to obesity-related lipid accumulation. Xu et al. found that the metabolic pathway of polysaccharides from Polygonatum cyrtonema polysaccharides intervening in obesity included glycerophospholipid metabolism, which is similar to the results of this study (52). The modulation of glycerophospholipid metabolism by AAEO likely involves the regulation of phosphatidylcholine and lysophosphatidylcholine levels, which are critical for triglyceride transport and membrane lipid homeostasis. Xu et al. (53) found through serum metabolomics analysis that patients with mild hypercholesterolemia have four potential metabolic pathways after consuming oats, namely glycerophospholipid metabolism, alanine, aspartic acid and glutamate metabolism, sphingolipid metabolism, and retinol metabolism. So, the mechanism of Artemisia argyi essential oil regulating obesity is related to the enrichment pathways mentioned above. In summary, the differential metabolites screened in this study are involved in the metabolic process of HFD induced obesity, which may be potential biomarkers regulating obesity. Further in-depth analysis of the metabolic mechanism of AAEO regulating obesity is expected to provide new research directions for improving obesity.

5 Conclusion

In summary, this study suggested that although AAEO induced selective changes in fecal microbial functions related to amino acid and lipid metabolism, while no significant shifts were observed in global microbiota composition in HFD induced obese mice, it can alter serum metabolites in ICR mice, which were mainly related to lipid metabolism. Through metabolic pathway identification, it was shown that AAEO mainly altered the linoleic acid metabolism and

glycerophospholipid metabolism pathway in mice and intervened in mice lipid metabolism.

Data availability statement

The metabolomics data have been deposited in the National Genomics Data Center (NGDC) under accession number PRJCA046608: https://ngdc.cncb.ac.cn/bioproject/browse/PRJCA046608.

Ethics statement

The animal study was approved by the Institutional Animal Care and Use Committee of Hunan Agricultural University. The study was conducted in accordance with the local legislation and institutional requirements.

Author contributions

KW: Writing – original draft, Data curation, Investigation. AY: Investigation, Software, Writing – review & editing. YL: Writing – review & editing, Data curation. QH: Writing – review & editing, Data curation. SX: Data curation. ZY: Writing – review & editing, Data curation. SX: Data curation, Writing – review & editing. JC: Supervision, Writing – review & editing, Investigation, Data curation, Software, Conceptualization, Methodology. PB: Writing – review & editing, Investigation, Conceptualization.

Funding

The author(s) declare that financial support was received for the research and/or publication of this article. This work was supported by ESI Discipline Special Project of Changsha Medical University (No.2022CYY006).

References

- 1. Haththotuwa RN, Wijeyaratne CN, Senarath U. Chapter 1—Worldwide epidemic of obesity. In: Mahmood TA, Arulkumaran S, Chervenak FA, editors. *Obesity and Obstetrics*. Amsterdam: Elsevier (2020). p. 3–8. doi: 10.1016/B978-0-12-817921-5.00001-1
- 2. Santos AL, Sinha S. Obesity and aging: molecular mechanisms and therapeutic approaches. *Ageing Res Rev.* (2021) 67:101268. doi: 10.1016/j.arr.2021. 101268
- 3. Castro AV, Kolka CM, Kim SP, Bergman RN. Obesity, insulin resistance and comorbidities? Mechanisms of association. *Arq Bras Endocrinol Metabol.* (2014) 58:600–9. doi: 10.1590/0004-2730000003223
- 4. Bao MH, Luo HQ, Chen LH, Tang L, Ma KF, Xiang J, et al. Impact of high fat diet on long non-coding RNAs and messenger RNAs expression in the aortas of ApoE(-/-) mice. *Sci Rep.* (2016) 6:34161. doi: 10.1038/srep34161
- 5. Xia Y, Huang CX, Li GY, Chen KH, Li H, Tang L, et al. Meta-analysis of the association between MBOAT7 rs641738, TM6SF2 rs58542926 and nonalcoholic fatty liver disease. *Clin Res Hepatol Gastroenterol.* (2019) 43:533–41. doi: 10.1016/j.clinre.2019.01.008
- 6. Ren WK, Xia YY, Chen SY, Wu GY, Bazer FW, Zhou BY, et al. Glutamine metabolism in macrophages: a novel target for obesity/type 2 diabetes. *Adv Nutr.* (2019) 10:321–30. doi: 10.1093/advances/nmy084

Conflict of interest

The authors declare that the research was conducted in the absence of any commercial or financial relationships that could be construed as a potential conflict of interest.

Generative AI statement

The author(s) declare that no Gen AI was used in the creation of this manuscript.

Any alternative text (alt text) provided alongside figures in this article has been generated by Frontiers with the support of artificial intelligence and reasonable efforts have been made to ensure accuracy, including review by the authors wherever possible. If you identify any issues, please contact us.

Publisher's note

All claims expressed in this article are solely those of the authors and do not necessarily represent those of their affiliated organizations, or those of the publisher, the editors and the reviewers. Any product that may be evaluated in this article, or claim that may be made by its manufacturer, is not guaranteed or endorsed by the publisher.

Supplementary material

The Supplementary Material for this article can be found online at: https://www.frontiersin.org/articles/10.3389/fnut.2025. 1650976/full#supplementary-material

- 7. Popkin BM. Synthesis and implications: China's nutrition transition in the context of changes across other low- and middle-income countries. *Obes Rev.* (2014) 15(Suppl 1):60–7. doi: 10.1111/obr.12120
- 8. Beslay M, Srour B, Mejean C, Alles B, Fiolet T, Debras C, et al. Ultra-processed food intake in association with BMI change and risk of overweight and obesity: a prospective analysis of the French NutriNet-Santé cohort. *PLoS Med.* (2020) 17:e1003256. doi: 10.1371/journal.pmed.1003256
- 9. Jiang CQ, Xu L, Zhang WS, Jin YL, Zhu F, Cheng KK, et al. Adiposity and mortality in older Chinese: an 11-year follow-up of the Guangzhou Biobank cohort study. *Sci Rep.* (2020) 10:1924. doi: 10.1038/s41598-020-58633-z
- 10. Mi B, Wu C, Gao X, Wu W, Du J, Zhao Y, et al. Long-term BMI change trajectories in Chinese adults and its association with the hazard of type 2 diabetes: evidence from a 20-year China Health and Nutrition Survey. *BMJ Open Diabetes Res Care.* (2020) 8:e000879. doi: 10.1136/bmjdrc-2019-000879
- 11. Pang Y, Kartsonaki C, Guo Y, Chen Y, Yang L, Bian Z. et al. Adiposity and risks of colorectal and small intestine cancer in Chinese adults: a prospective study of 05 million people. *Br J Cancer*. (2018) 119:248–50. doi: 10.1038/s41416-018-0124-8
- 12. Oussaada SM, van Galen KA, Cooiman MI, Kleinendorst L, Hazebroek EJ, van Haelst MM, et al. The pathogenesis of obesity. *Metabolism.* (2019) 92:26–36. doi: 10.1016/j.metabol.2018.12.012

- 13. Kakkar AK, Dahiya N. Drug treatment of obesity: current status and future prospects. Eur J Intern Med. (2015) 26:89–94. doi: 10.1016/j.ejim.2015.01.005
- 14. Khera R, Murad MH, Chandar AK, Dulai PS, Wang Z, Prokop LJ, et al. Association of pharmacological treatments for obesity with weight loss and adverse events: a systematic review and meta-analysis. *JAMA*. (2016) 315:2424–34. doi: 10.1001/jama.2016.7602
- 15. Kim GW, Lin JE, Blomain ES, Waldman SA. Antiobesity pharmacotherapy: new drugs and emerging targets. *Clin Pharmacol Ther*. (2014) 95:53–66. doi:10.1038/clpt.2013.204
- 16. Abad MJ, Bedoya LM, Apaza L, Bermejo P. The artemisia L. Genus: a review of bioactive essential oils Molecules. (2012) 17:2542–66. doi: 10.3390/molecules17032542
- 17. Chen LL, Zhang HJ, Chao J, Liu JF. Essential oil of Artemisia argyi suppresses inflammatory responses by inhibiting JAK/STATs activation. *J Ethnopharmacol.* (2017) 204:107–17. doi: 10.1016/j.jep.2017.04.017
- 18. Ge YB, Wang ZG, Xiong Y, Huang XJ, Mei ZN, Hong ZG. Anti-inflammatory and blood stasis activities of essential oil extracted from Artemisia argyi leaf in animals. *J Nat Med.* (2016) 70:531–8. doi: 10.1007/s11418-016-0972-6
- 19. Zhang WJ, You CX, Yang K, Chen R, Wang Y, Wu Y, et al. Bioactivity of essential oil of Artemisia argyi Lévl. et Van and its main compounds against Lasioderma serricorne. J Oleo Sci. (2014) 63:829–37. doi: 10.5650/jos.ess14057
- 20. Li N, Mao Y, Deng C, Zhang X. Separation and identification of volatile constituents in Artemisia argyi flowers by GC-MS with SPME and steam distillation. *J Chromatogr Sci.* (2008) 46:401–5. doi: 10.1093/chromsci/46.5.401
- Wenqiang G, Shufen L, Ruixiang Y, Yanfeng H. Comparison of composition and antifungal activity of Artemisia argyi Levl. et Vant inflorescence essential oil extracted by hydrodistillation and supercritical carbon dioxide. *Nat Prod Res.* (2006) 20:992–8. doi: 10.1080/14786410600921599
- 22. Lu XF, Zhou Y, Zhang J, Ren YP. Determination of fluoroquinolones in cattle manure-based biogas residue by ultrasonic-enhanced microwave-assisted extraction followed by online solid phase extraction-ultra-high performance liquid chromatography-tandem mass spectrometry. *J Chromatogr B Analyt Technol Biomed Life Sci.* (2018) 1086:166–75. doi: 10.1016/j.jchromb.2018.01.029
- 23. Campelo-Felix PH, Souza HJ, Figueiredo JA, Fernandes RV, Botrel DA, de Oliveira CR, et al. Prebiotic carbohydrates: effect on reconstitution, storage, release, and antioxidant properties of lime essential oil microparticles. *J Agric Food Chem.* (2017) 65:445–53. doi: 10.1021/acs.jafc.6b04643
- 24. Mojtahed Zadeh Asl R, Niakousari M, Hashemi Gahruie H, Saharkhiz MJ. Mousavi Khaneghah A. Study of two-stage ohmic hydro-extraction of essential oil from Artemisia aucheri Boiss: antioxidant and antimicrobial characteristics. *Food Res Int.* (2018) 107:462–9. doi: 10.1016/j.foodres.2018.02.059
- 25. Yun C, Jung Y, Chun W, Yang B, Ryu J, Lim C, et al. Anti-inflammatory effects of artemisia leaf extract in mice with contact dermatitis in vitro and in vivo. *Mediators Inflamm.* (2016) 2016:8027537. doi: 10.1155/2016/8027537
- 26. Shi GX, Wang TM, Wu SB, Wang YX, Shao J, Zhou MQ, et al. [Activity of essential oil extracted from Artemisia argyi in inducing apoptosis of Candida albicans]. *Zhongguo Zhong Yao Za Zhi.* (2017) 42:3572–7. doi: 10.19540/j.cnki.cjcmm.2017.0136
- 27. Loziene K, Svediene J, Paskevicius A, Raudoniene V, Sytar O, Kosyan A. Influence of plant origin natural alpha-pinene with different enantiomeric composition on bacteria, yeasts and fungi. *Fitoterapia*. (2018) 127:20–4. doi: 10.1016/j.fitote.2018.04.013
- 28. Editorial Board of Chinese Pharmacopoeia. Chinese Pharmacopoeia. Vol. 1, Beijing: Chemistry and Industry Press (2015). p. 89.
- 29. Huang HC, Wang HF, Yih KH, Chang LZ, Chang TM. Dual bioactivities of essential oil extracted from the leaves of as an antimelanogenic antioxidant agent and chemical composition analysis by GC/MS. *Int J Mol Sci.* (2012) 13:14679–97. doi: 10.3390/ijms131114679
- 30. Bao X, Yuan H, Wang C, Liu J, Lan M. Antitumor and immunomodulatory activities of a polysaccharide from Artemisia argyi. *Carbohydr Polym.* (2013) 98:1236–43. doi: 10.1016/j.carbpol.2013.07.018
- 31. Chen JY, Chen FM, Peng SM, Ou YJ, He BS, Li YH, et al. Effects of *Artemisia argyi* powder on egg quality, antioxidant capacity, and intestinal development of roman laying hens. *Front Physiol* (2022) 13:902568. doi: 10.3389/fphys.2022.902568
- 32. Pan JG, Xu ZL, Ji L. Chemical studies on essential oils from 6 Artemisia species. *Zhongguo Zhong Yao Za Zhi*. (1992) 17:741–4, 64.

- 33. Wang K, Ma J, Li Y, Han Q, Yin Z, Zhou M, et al. Effects of essential oil extracted from Artemisia argyi leaf on lipid metabolism and gut microbiota in high-fat diet-fed mice. *Front Nutr.* (2022) 9:1024722. doi: 10.3389/fnut.2022.1024722
- 34. Wang K, Zhou M, Gong X, Zhou Y, Chen J, Ma J, et al. Starch–protein interaction effects on lipid metabolism and gut microbes in host. *Front Nutr.* (2022) 9:1018026. doi: 10.3389/fnut.2022.1018026
- 35. Chen F, Wang Y, Wang K, Chen J, Jin K, Peng K, et al. Effects of Litsea cubeba essential oil on growth performance, blood antioxidation, immune function, apparent digestibility of nutrients, and fecal microflora of pigs. *Front Pharmacol.* (2023) 14:1166022. doi: 10.3389/fphar.2023.1166022
- 36. Wang K, Yang A, Peng X, Lv F, Wang Y, Cui Y, et al. Linkages of various calcium sources on immune performance, diarrhea rate, intestinal barrier, and post-gut microbial structure and function in piglets. *Front Nutr.* (2022) 9:921773. doi: 10.3389/fnut.2022.921773
- 37. Wang KJ, Yan QX, Ren A, Zheng ML, Zhang PH, Tan ZL, et al. Novel linkages between bacterial composition of hindgut and host metabolic responses to sara induced by high-paddy diet in young goats. *Front Vet Sci.* (2022) 8:791482. doi: 10.3389/fvets.2021.791482
- 38. Kotnis MS, Patel P, Menon SN, Sane RT. Renoprotective effect of Hemidesmus indicus, a herbal drug used in gentamicin-induced renal toxicity. *Nephrology (Carlton)*. (2004) 9:142–52. doi: 10.1111/j.1440-1797.2004.00247.x
- 39. Chan K. Some aspects of toxic contaminants in herbal medicines. Chemosphere. (2003) 52:1361–71. doi: 10.1016/S0045-6535(03)00471-5
- 40. Jinxin M, Xiaofang G, Mingsan M. External curative effect of mugwort water decoction in pruritus and dermatitis model. *Pharmacol Clin Chin Mater Med.* (2012) 28:117–9. doi: 10.13412/j.cnki.zyyl.2012.05.077
- 41. Jiang Z-T, Tan J, Tan J, Li R. Chemical components and molecular microcapsules of folium Artemisia argyi essential oil with β -cyclodextrin derivatives. *J Essent Oil Bear Plants*. (2016) 19:1155–69. doi: 10.1080/0972060X.2016.1185973
- 42. Ehrnhöfer-Ressler MM, Fricke K, Pignitter M, Walker JM, Walker J, Rychlik M, et al. Identification of 1,8-cineole, borneol, camphor, and thujone as anti-inflammatory compounds in a *Salvia officinalis L*. infusion using human gingival fibroblasts. *J Agric Food Chem.* (2013) 61:3451–9. doi: 10.1021/jf305472t
- 43. Miguel MG. Antioxidant and anti-inflammatory activities of essential oils: a short review. *Molecules*. (2010) 15:9252–87. doi: 10.3390/molecules15129252
- 44. Zongguo H, Haisheng W, Lingling Z, Feng L, Huangan W. (2013). Study on the yield and chemical components of the volatile oil from Artemisiae argyi levl. et vant. gathered in different growing period. *J South-Central Univ Nation*. (2013) 32:32–35.
- 45. Lan M-B, Yu Y-L, Li X-H. Analysis on the chemical constituents of the essential oil of Artemisia argyi levl. et vant. in Guizhou. *Chin J Pharm Ana*. (2009) 29:1305–8.
- 46. Zheng-You HE, Yan-Hong Z, Dong W, Rong-Hua YU, Hui-Hui Y, Min-Bo L. Chemical composition of essential oil from fresh and dried folium Artemisia argyi from Hubei province. *Chin Tradit Pat Med.* (2009) 31:1079–82.
- 47. He BS, Zhu RR, Yang HD, Lu QQ, Wang WW, Song L, et al. Assessing the impact of data preprocessing on analyzing next generation sequencing data. *Front Bioeng Biotechnol.* (2020) 8:817. doi: 10.3389/fbioe.2020.00817
- 48. Liu S, Wang KJ, Lin SZ, Zhang ZD, Cheng M, Hu SS, et al. Comparison of the effects between tannins extracted from different natural plants on growth performance, antioxidant capacity, immunity, and intestinal flora of broiler chickens. *Antioxidants*. (2023) 12:441. doi: 10.3390/antiox12020441
- 49. Fanos V, Pintus R, Dessi A. Clinical metabolomics in neonatology: from metabolites to diseases. *Neonatology.* (2018) 113:406–13. doi: 10.1159/000487620
- 50. Johnson CH, Ivanisevic J, Siuzdak G. Metabolomics: beyond biomarkers and towards mechanisms. Nat Rev Mol Cell Biol. (2016) 17:451–9. doi: 10.1038/nrm.2016.25
- 51. Scalbert A, Brennan L, Manach C, Andres-Lacueva C, Dragsted LO, Draper J, et al. The food metabolome: a window over dietary exposure. *Am J Clin Nutr.* (2014) 99:1286–308. doi: 10.3945/ajcn.113.076133
- 52. Xu RJ. The Effect of Polygonatum Cyrtonema Polysaccharide on Nutritional Obesity Based on Metabolomics. Hefei: Anhui University of Chinese Medicine (2021).
- 53. Xu D, Wang S, Feng M, Shete V, Chu Y, Kamil A, et al. Serum Metabolomics reveals underlying mechanisms of cholesterol-lowering effects of oat consumption: a randomized controlled trial in a mildly hypercholesterolemic population. *Mol Nutr Food Res.* (2021) 65:e2001059. doi: 10.1002/mnfr.202001059